

## Physical Optics and the Impedance Boundary Condition

Edwin Okoampa Boadu<sup>1</sup>, Kingsford Kissi Mireku<sup>2</sup>, KomlanGbongli<sup>3</sup>

<sup>1</sup>(Faculty of Allied Sciences, Koforidua Technical University, Ghana)

<sup>2</sup>(Information and Software Engineering, University of Electronic, Science and Technology of China, China)

<sup>3</sup>(School of Management and Economics, University of Electronic, Science and Technology of China, China)

**ABSTRACT:** Wave propagation is an important phenomenon in the context of mobile systems. From basic diffraction one can develop methods for objects that are used as models for obstacles in the path of propagation. In order to combine a number of objects, the method known as Physical Optics can be used. This method is mostly used for perfectly conducting surfaces but can be extended to surfaces described by means of an impedance boundary condition. It will be shown that targets that have impedance surfaces yield RCS results that are lower than the results of perfectly conducting surfaces. The results obtained are compared with exact methods and other approximation methods and they are in good agreement. Application of these results to stealth technology and wave propagation is discussed.

**Keywords:** Physical Optics, Impedance Boundary Condition (IBC), Radar Cross Section (RCS), Monostatic and Bistatic

### I. INTRODUCTION

Wave propagation is an important phenomenon in the context of mobile systems or mobile communication. However, because of the irregular nature of the ground and obstacles in the path of propagation, there are scattering issues involved. When a perfectly conducting body is illuminated by an electromagnetic wave, electric currents are induced on the surface of the body. These currents act as new sources and create an electromagnetic field radiated outward from the body.

These new electromagnetic fields are the scattered fields. In order to evaluate the amount of waves that are scattered, the scattered electric and magnetic field must be computed. Knowing these entities one may compute the radar cross section (RCS), which describes the electromagnetic scattering properties of a target. The calculation of the RCS for plane wave illumination is of great practical and academic interest, since complex radar targets and wave propagation models can be studied with the results. There are numerous methods to calculate the scattered fields. We have the high frequency methods and various more or less numerical methods [1]. Among the high frequency methods, we have geometrical optics (GO), the geometrical theory of diffraction (GTD) and physical optics (PO) with their derivatives. In this study, we concentrate on the extension of physical optics.

Physical optics is an approximate method for the determination of the field scattered by an object through an assumption about the specific form of the field distribution on the surface. It is assumed that at each point on the geometrically illuminated side of the body the scattering at the surface takes place as though from an infinite tangent plane at the point. Over the shadow portion of the body the surface field is assumed to be zero.

The physical optics approximation is known to provide results that are in good agreement with both experiments and exact theoretical solutions. Physical optics is mostly used to solve scattering problems involving perfectly conducting objects but can be extended to problems involving imperfectly conducting objects that are described by means of an impedance boundary condition.

### II. PROBLEM DEFINITION

The scattering problem in wave propagation often comes under the heading of computational electromagnetism and has been investigated extensively over the years. Many researchers have attempted to explain the nature of light and its interaction with matter or particles. Much of this work can be carried over to radar scattering problems because radio waves and light waves are merely two forms of the same electromagnetic phenomenon.

Perfectly conducting surfaces are the most common application of physical optics and the relative impedance of the surface is then zero which makes calculations easier. If the relative surface impedance varies over the surface, complications arise and it is hence often assumed to be constant in space and time [2]. Scattering from bodies with imperfectly conducting surfaces is central to many problems in optics and in the study of wave propagation models. Imperfectly conducting characterize many non-metallic scatters.

Physical optics and its advantages have been briefly introduced. This research will investigate an imperfectly conducting sphere with an impedance boundary condition by means of an extension of physical optics. Both monostatic and bistatic cases are considered.

In order to establish notation, the fundamentals of electromagnetics are presented in this study. Maxwell's equations are a set of fundamental equations that govern all macroscopic electromagnetic phenomena. The differential form of these equations is given and used in the subsequent sections. Maxwell's equations in the differential form can be derived from the integral form by using Gauss's and Stokes's theorems. For a point in space where all the field quantities and their derivatives are continuous, one obtains [3]:

$$\nabla \times \vec{E} = - \frac{\partial \vec{B}}{\partial t} \quad \text{(Faraday's law) (1)}$$

$$\nabla \times \vec{H} = \frac{\partial \vec{D}}{\partial t} + \vec{J} \quad \text{(Maxwell-Ampere law) (2)}$$

$$\nabla \cdot \vec{J} = - \frac{\partial \rho}{\partial t} \quad \text{(Equation of continuity) (3)}$$

$$\nabla \cdot \vec{D} = \rho \quad \text{(Gauss's law) (4)}$$

$$\nabla \cdot \vec{B} = 0 \quad \text{(Gauss's law - magnetic) (5)}$$

Time-Harmonic Fields: when the field quantities in Maxwell's equations are harmonically oscillating functions with a single frequency, the field is referred to as time-harmonic. Using the complex phasor notation, equation 1, 2 and 3 can be written in simplified form as:

$$\nabla \times \vec{E} = j \omega \vec{B} \quad (6)$$

$$\nabla \times \vec{H} = -j \omega \vec{D} + \vec{J} \quad (7)$$

$$\nabla \cdot \vec{J} = -j \omega \rho \quad (8)$$

The phasor factor  $e^{-j\omega t}$  is used here, where  $\omega$  is the angular frequency. It is evident in this case that the electric and the magnetic fields must exist simultaneously and interact with each other. It is also evident that the static case is the limiting case of the harmonic fields as the frequency  $\omega$  approaches zero. For isotropic materials the following so-called constitutive relations apply:

$$\vec{D} = \epsilon_0 \epsilon_r \vec{E} \quad (9)$$

$$\vec{B} = \mu_0 \mu_r \vec{H} \quad (10)$$

The constant  $\epsilon_0 = 8.854 \times 10^{-12} \text{ farad/meter}$  is the permittivity for vacuum and  $\epsilon_r$  is the relative permittivity. Similarly  $\mu_0 = 4\pi \times 10^{-7} \text{ henry/meter}$  and  $\mu = \mu_0 \mu_r$  is the magnetic permeability. The total field used in the formulation of the scattered field and the boundary condition given in equation 19 must satisfy the following Maxwell's field equations2:

$$\nabla \times \vec{E} = -j \omega \mu \vec{H} = -j k Z_0 \eta_w \vec{H} \quad (11)$$

$$\nabla \times \vec{H} = j \omega \epsilon \vec{E} = j \frac{k}{Z_0 \eta_w} \vec{E} \quad (12)$$

where the relative wave impedance for the material is  $\eta_w = \sqrt{\mu_r / \epsilon_r}$ ,  $Z_0 = \sqrt{\mu_0 / \epsilon_0} = 120\pi$  is the wave impedance for vacuum and  $k = \omega \sqrt{\mu \epsilon}$  is the wave number.

Boundary Conditions, complete description of an electromagnetic problem should include information about both the differential equations and the boundary conditions that can be derived from Maxwell's equations in integral form. At the Interface between Two Media, a source-free interface between medium 1 and medium 2, the fields must satisfy these four conditions:

$$\hat{n} \times (\vec{E}_1 - \vec{E}_2) = 0 \tag{13}$$

$$\hat{n} \cdot (\epsilon_1 \vec{E}_1 - \epsilon_2 \vec{E}_2) = 0 \tag{14}$$

$$\hat{n} \times (\vec{H}_1 - \vec{H}_2) = 0 \tag{15}$$

$$\hat{n} \cdot (\mu_{r1} \vec{H}_1 - \mu_{r2} \vec{H}_2) = 0 \tag{16}$$

Where  $\epsilon_{1,2} = \epsilon' - j\epsilon''$ .  $\hat{n}$  is the unit vector normal to the interface pointing away from medium 2 into medium 1 as in Fig. 2.1. These relations are also known as the field continuity conditions.

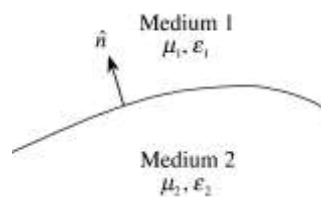


Figure 2.1 Interface between two media.

At a Perfectly Conducting Surface, the boundary conditions can be simplified when one of the media, Example medium 2, is a perfect conductor. Since a perfect conductor cannot sustain internal fields, equation 13 and 16 become:

$$\hat{n} \times \vec{E}_1 = 0 \tag{17}$$

$$\hat{n} \cdot \vec{B}_1 = 0 \tag{18}$$

$\vec{E}_1$  and  $\vec{B}_1$  are the fields exterior to the conductor and  $\hat{n}$  is the normal vector pointing away from the conductor. In this case the boundary can always support a surface current  $\vec{j}_s = \hat{n} \times \vec{H}$  and a surface charge ( $\rho_s = \hat{n} \cdot \vec{D}$ )

For an Imperfectly Conducting, when medium 2 is an imperfect conductor, it can be shown that the electric and the magnetic fields at the surface of the conductor are approximately related by equation 4 and 5:

$$\vec{E} - (\hat{n} \cdot \vec{E}) \hat{n} = \eta Z_0 \hat{n} \times \vec{H} \tag{19}$$

$$\hat{n} \times \vec{E} = \eta Z_0 \left[ (\hat{n} \cdot \vec{H}) \hat{n} - \vec{H} \right] \tag{20}$$

Equations 19 or 20 are referred to as an impedance boundary condition (IBC).

### III. RADAR CROSS SECTION

An important parameter that characterizes scattering by an object is the Radar Cross Section (RCS). It is a measure of the power that is returned or scattered in a given direction normalized with respect to the power density of the incident field. RCS is defined as the area required to be cut out of the incident wave front at the position of the scatterer, so that the power thereby intercepted would, if radiated isotopically, create the same power density at the observation point as does the scatterer [6]. The Radar Cross Section defined for plane-wave incidence and in three dimensions is given by [6]:

$$\sigma(\theta, \phi, \theta^i, \phi^i) = \lim_{r \rightarrow \infty} 4\pi r^2 \frac{|E^{sc}(r, \theta, \phi)|^2}{|E^i(\theta^i, \phi^i)|^2} \tag{21}$$

$E^{sc}$  denotes the scattered field observed in the direction  $(\theta, \phi)$  and  $E^i$  denotes the incident field from the direction  $(\theta^i, \phi^i)$ . When the incident and observation directions coincide,  $\sigma$  is called the monostatic or backscattering RCS, otherwise, it is referred to as the bistatic RCS. To incorporate information about polarization, the radar cross section is defined as [6]:

$$\sigma_{p,q}(\theta, \phi, \theta^i, \phi^i) = \lim_{r \rightarrow \infty} 4\pi r^2 \frac{|E_p^{sc}(r, \theta, \phi)|^2}{|E_q^i(\theta^i, \phi^i)|^2} \quad (22)$$

Where P and q represent the field components, referring to either  $\theta$  or  $\phi$ .

Polarization relates to the components in equation 22. The polarization of an electromagnetic wave is defined in terms of the orientation of the electric field vector. The electric field vector is always perpendicular to both the direction of travel and the magnetic field vector. The polarization is described by the geometric figure traced by the electric field vector upon a stationary plane perpendicular to the direction of propagation [7], as the wave travels through that plane. An electromagnetic wave is frequently composed of (or can be broken down into) two orthogonal components. Depending on the path traced by the electric field vector, we either have linear polarization, circular polarization or elliptical polarization. Linear polarization is used here and it is given by  $\hat{a}$  in equation 27.

#### IV. FORMULATION AND COMPUTATION

In formulating equations to compute the radar cross section of a body, whose characteristic dimension is greater than the wavelength of the incident radiation, the physical optics approximation can be used.

It is interesting to extend this method so as to approximate the radar cross section of imperfectly conducting scatterers with an impedance boundary condition. If a body is not perfectly conducting there is the possibility of formulating an impedance boundary condition at the surface. This condition, given by equation 19, allows one to determine the external electromagnetic field without explicitly considering the field inside the body [2].

#### V. VALIDITY OF THE IMPEDANCE BOUNDARY CONDITION:

In order for the impedance boundary condition to be accurate one requires that:

1. The absolute value of the relative complex refractive index of the material of the scatterer must be large compared to unity.
2. The radius of curvature of the surface of the body must be large compared to both the penetration of the inward traveling field and the inverse of the absolute value of the wave number inside the body.

Physical Optics uses the following steps in order to find the scattered field.

1. The current excited on the surface of the scatterer is given by the tangential components of the incident fields on the surface. Since the field is assumed to exist only on the illuminated portions of the scattering body, the PO current for a perfectly conducting body is given by [1]:

$$\vec{J}_s = \begin{cases} 2 \hat{n} \times \vec{H}^i & \text{lit region,} \\ 0 & \text{shadow} \end{cases} \quad (23)$$

Where  $\hat{n}$  the unit is normal vector pointing outward and  $\vec{H}^i$  is the incident magnetic field.

2. Using radiation integrals, the PO surface current is integrated over the surface of the scatterer to yield the scattered field.

In a Scattered far – field, a plane incident electromagnetic wave is defined by:

$$\vec{E}^i = \hat{a} e^{ik(\hat{k} \cdot \vec{r}) - i\omega t} \quad (24)$$

$$\vec{H}^i = \frac{1}{Z_0} \hat{b} e^{ik(\hat{k} \cdot \vec{r}) - i\omega t}, \quad \hat{b} = \hat{k} \times \hat{a} \quad (25)$$

where t is the time,  $\omega$  is the angular frequency,  $k = \frac{2\pi}{\lambda} = \omega \sqrt{\mu_0 \epsilon_0}$  is the free space wave number, and  $\vec{r}$  is the vector from an origin O located somewhere inside the body to a point Q on the illuminated surface  $S_i$  with the unit normal  $\hat{n}$ .

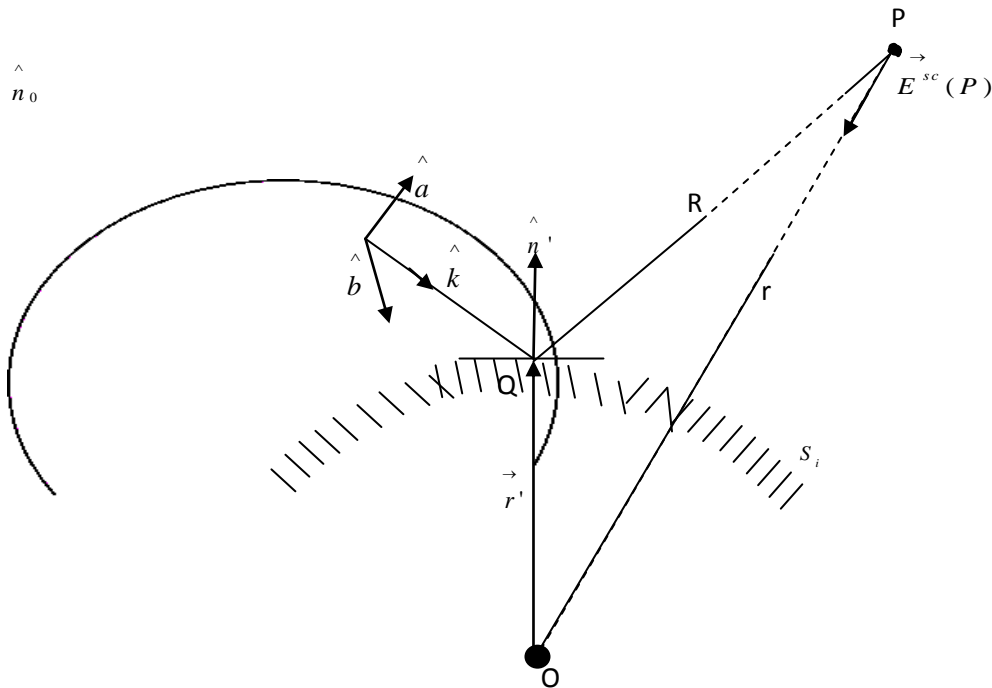


Figure 3.1 Basic geometry for the scattering problem.

In the physical optics approximation, the scattered field  $\vec{E}^{sc}$  at a point P very far from the body is given by the formula [2] and [8]:

$$\vec{E}^{sc}(P) = \frac{1}{4\pi} \iint_{S_i} i\omega\mu_0 (\hat{n}' \times \vec{H}(r')) G + (\hat{n}' \times \vec{E}(r')) \times \nabla G dS_i' \tag{26}$$

$$G = \frac{e^{ikR}}{R}, \quad R = \left| \vec{r} - \vec{r}' \right| \tag{27}$$

Using vector identities and Maxwell's equations one obtains the scattered field from a surface with an impedance  $\eta$  as in [2]:

$$\vec{E}^{sc}(P) \approx \frac{ie^{ikR}}{\lambda R} \iint_{S_i} \frac{\hat{n}' \cdot \hat{k}}{[\hat{k} \times \hat{n}']^2} f e^{ik\vec{r}' \cdot (\hat{n}_0 + \hat{k})} dS_i' \tag{28a}$$

Where

$$f = \frac{\hat{n}' \cdot \hat{a}}{\hat{n}' \cdot \hat{k} - \eta} \left[ (\hat{n}' + \eta \hat{n}_0) \times (\hat{k} \times \hat{n}') \right] + \frac{\hat{a} \cdot \hat{k} \times \hat{n}'}{\eta \hat{n}' \cdot \hat{k} - 1} \left[ \hat{k} \times \hat{n}' + \eta \left\{ \hat{n}' \times (\hat{k} \times \hat{n}') \right\} \times \hat{n}_0 \right] \tag{28b}$$

The radar cross section is then obtained using the relations in equation 3. Letting  $\eta$  equal to zero, one finds that equation 28 becomes:

$$\vec{E}^{sc}(P)_{\eta=0} = \frac{ie^{ikR}}{\lambda R} \iint_{S_i} (\hat{n}' \times \hat{b}) e^{ik \vec{r}' \cdot (\hat{n}_0 + \hat{k})} dS_i' \tag{29}$$

This is the well-known physical optics results for the bistatic cross section of a perfectly conducting body. In the Monostatic Radar Cross Section, by letting  $\hat{n}_0 = \hat{k}$  in equation 28 one obtains the backscattering result. The scattered far-field then reduces to [2]:

$$\vec{E}^{bs} \approx \frac{ie^{ikR}}{\lambda R} (G_1 \hat{a} + G_2 \hat{b}) \tag{30}$$

$$G_1 = \iint_{S_i} \frac{\hat{n}' \cdot \hat{k}}{\eta \hat{n}' \cdot \hat{k} - 1} \left[ 1 + \eta \hat{n}' \cdot \hat{k} + 2\eta \frac{(\hat{n}' \cdot \hat{a})^2}{\hat{n}' \cdot \hat{k} - \eta} \right] e^{i2k \vec{r}' \cdot \hat{k}} dS_i' \tag{31a}$$

$$G_2 = 2\eta \iint_{S_i} \hat{n}' \cdot \hat{k} \frac{(\hat{n}' \cdot \hat{a})(\hat{n}' \cdot \hat{b})}{(\hat{n}' \cdot \hat{k} - \eta)(1 - \eta \hat{n}' \cdot \hat{k})} e^{i2k \vec{r}' \cdot \hat{k}} dS_i' \tag{31b}$$

This gives a simpler cross section,

$$\sigma = \frac{4\pi}{\lambda^2} (|G_1|^2 + |G_2|^2) \tag{32}$$

Now let's look at one consequence of equation 30. Letting  $\eta$  equal to zero, one finds that equation 30 becomes:

$$\vec{E}^{bs} \approx -\frac{ie^{ikR}}{\lambda R} \hat{a} \iint_{S_i} \hat{n}' \cdot \hat{k} e^{i2k \vec{r}' \cdot \hat{k}} dS_i' \tag{33}$$

This is also the well-known physical optics results for the monostatic radar cross section of a perfectly conducting body.

It was mentioned initially that the aim is to compute the radar cross section of an imperfectly conducting sphere. Considering the rotational symmetry of a sphere,  $\hat{k}$  is set to  $-\hat{z}$  and  $\hat{a}$  is set to  $\hat{x}$ . This gives  $\hat{b} = \hat{y}$ . A point  $(a, \theta', \phi')$ , where  $\vec{a} = [r']$ , on the surface  $S_i$  has the unit normal  $\hat{n}'$  at that point.  $\hat{n}'$  and  $\vec{r}'$  are obtained explicitly as:

$$\hat{n}' = [\sin(\theta') \cos(\phi'), \sin(\theta') \sin(\phi'), \cos(\theta')] \tag{34}$$

$$\vec{r}' = a \hat{n}' \tag{35}$$

It is then straightforward to perform the integration in equation 28. By including the factor  $a^2 \sin(\theta')$  in the integrand one obtains a double integral suited to MATLAB [9]. The domain of integration is a spherical half shell in this case.

For smooth scatterers one could use the method of stationary phase to compute the PO integral in the high frequency limit and the result for the sphere is given as equation 36. This result was obtained with the condition that the illuminated surface of the scatterer is symmetric with respect to a plane parallel to the direction of propagation of the incident wave [2].

$$\sigma_{sphere} = \pi a^2 \left| \frac{1 - \eta}{1 + \eta} \right|^2 \tag{36}$$

By letting  $\eta = 0$  in equation 36 one recovers the high frequency limit for the perfectly conducting sphere. When  $\eta = 1$ ,  $\sigma_{sphere} = 0$  and this has implications for stealth technology.

### VI. RESULTS AND OBSERVATIONS

Several numerical examples are given to demonstrate the accuracy of the method of physical optics as it is extended to the case with impedance boundary conditions. The examples are chosen to include a number of

different relative surface impedances. The results are plotted in the form of monostatic RCS versus wave number and bistatic RCS versus angle.

Monostatic simulation scattering results for a sphere is presented in Figures 4.1 through 4.3 using the MATLAB scripts in Appendices A1, A2 and A3.

The incidence and the observation angles are chosen as  $\theta = \varphi = 0$  without loss of generality since the sphere is rotationally symmetric. In Figure 4.1, where the impedance is set to zero, a comparison is made with the exact Mie-series [8]. In both cases the solution tends to the value  $\pi a^2$ , i.e., the geometrical cross section of the sphere. The PO solution does not quite reproduce the resonances that are related to waves circling the sphere. The PO graphs in Figures 4.1 to 4.3 can be obtained using either equation 28 or equation 32. Figure 4.1 shows that the scattering has three domains. The low frequency or Rayleigh domain,  $ka < 0.4$ , the resonance domain,  $0.4 \leq ka \leq 20$ , and the optical domain,  $ka > 20$ .

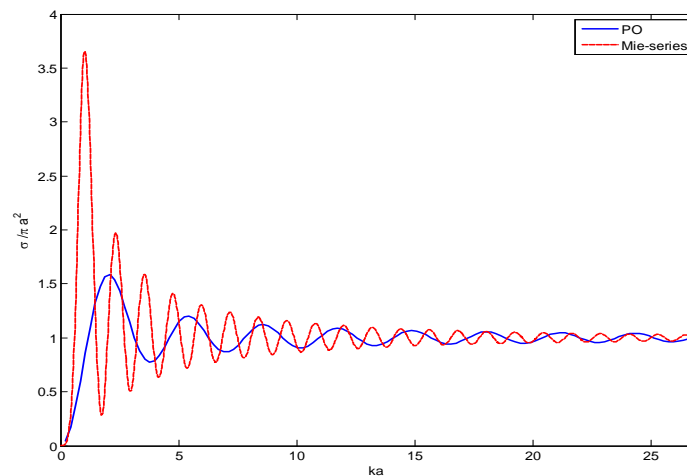


Figure 4.1 Monostatic Scattering RCS with  $\eta = 0$ . The exact solution is computed by means of the Mie-series.

Both complex and real values of the impedance are considered here. When  $\eta$  tends to one, as in Figure 4.2, the RCS tends to zero as expected from the high frequency asymptote given in equation 36. The relative impedance can be larger than one and this will again give large cross sections. For complex impedances there is also absorption in the sphere and this affects the cross section.

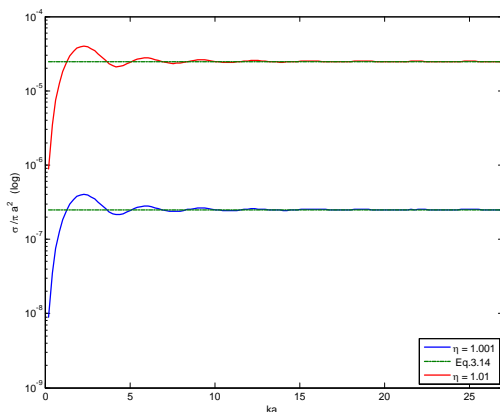


Figure 4.2 Monostatic Scattering RCS for real  $\eta$  close to unity

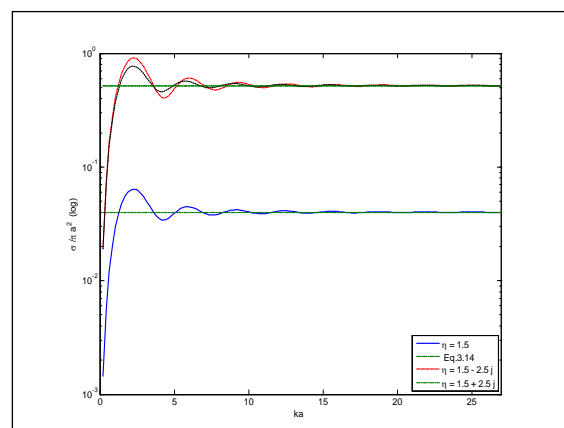


Figure 4.3 Monostatic Scattering RCS for complex  $\eta$ .

Bistatic simulation results: Figures 4.4 to 4.7 (Appendix A3) present the bistatic radar cross section for the sphere for an incident wave as indicated in Figure 3.1 and equation 24. The angles of incidence are  $\theta^i = 0$  and  $\theta^i = 0$  or  $\pi/2$ . The observation angle  $\theta$  is varied over the range  $0$  to  $\pi$  and the observation angle  $\varphi$  is constant at  $0$  or  $\pi/2$ . It is observed that the RCS is largest at  $\theta = \pi$ . This angle is called the forward scattering direction. There is a strong lobe in the forward direction and this lobe combines with the incident field to form the shadow. For high frequencies they cancel and produce a well-defined shadow. Results for a variety

of impedances are given without comparison to exact results or other methods due to the limited scope of this investigation.

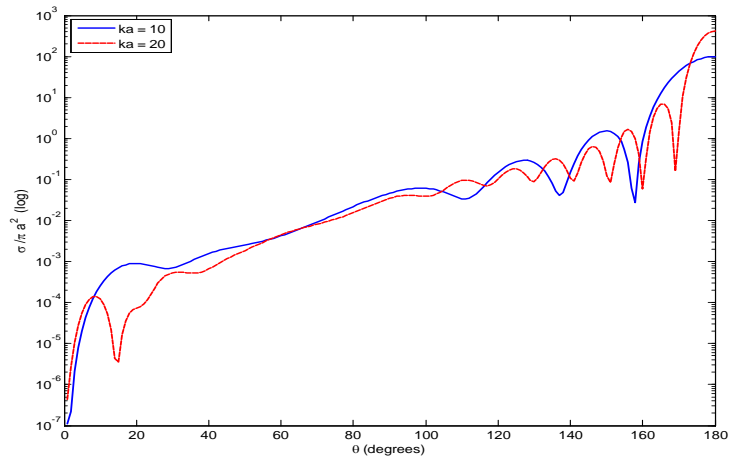


Figure 4.4 Bistatic Scattering RCS when  $\eta = 1.001$ .

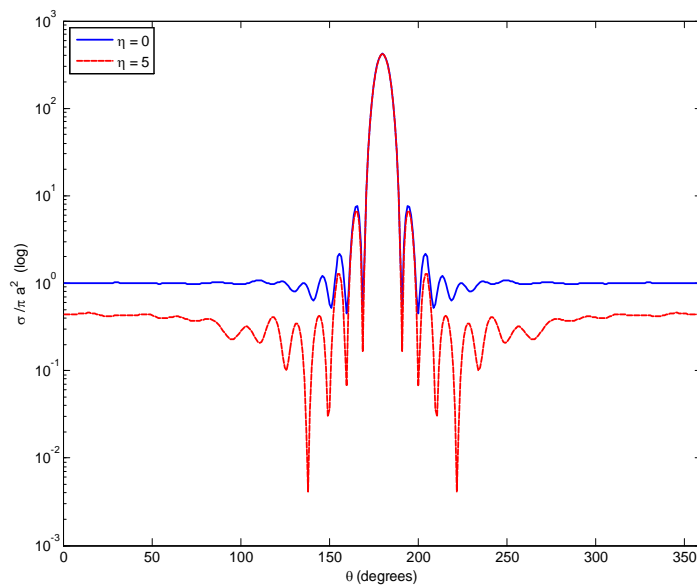
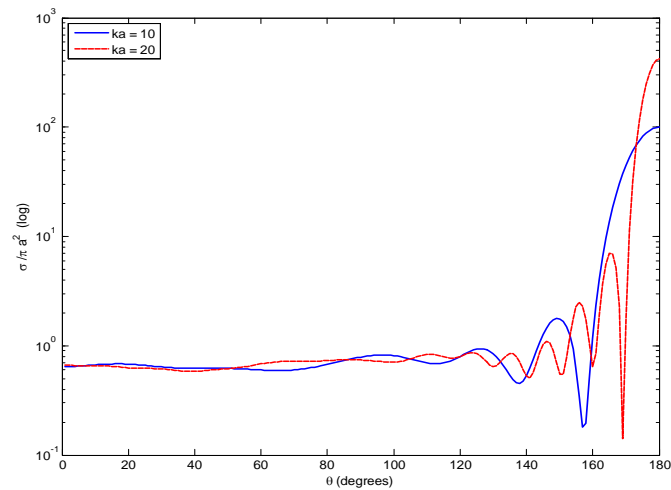
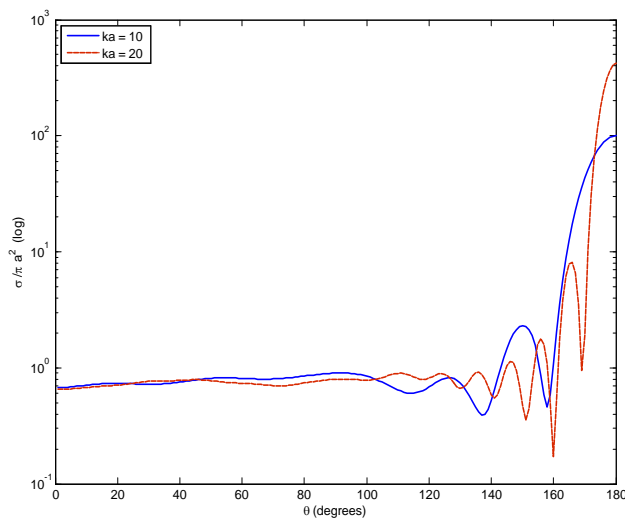


Figure 4.5 Bistatic Scattering RCS for real  $\eta$  when  $ka = 20$ .





(a)



(b)

Figure 4.6 Bistatic Scattering RCS when (a)  $\eta=0.1-0.1j$  (b)  $\eta=0.1+0.1j$ .

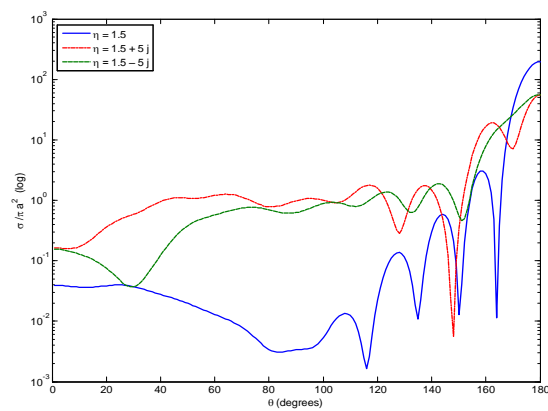
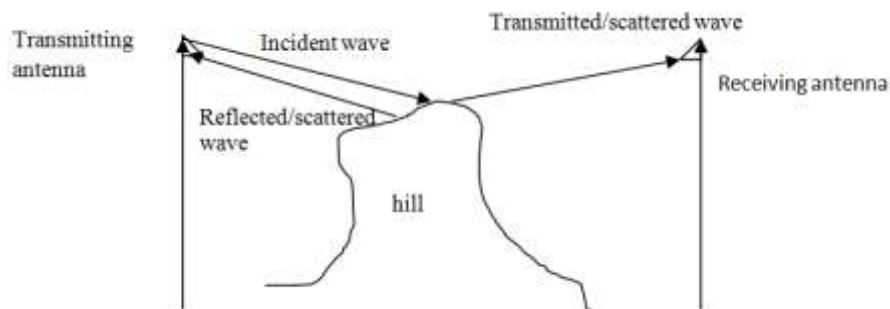


Figure 4.7 Bistatic Scattering RCS for complex  $\eta$  when  $ka=14$ .

## VII. APPLICATIONS OF THE RADAR CROSS SECTION

Researchers have known for nearly 100 years that objects reflect radio waves, but it was not until the advent of radar during World War II that these reflections really came to the fore. Even though the simulation of radar cross section can be very complex, a simple object such as the imperfectly conducting sphere and a simple method such as physical optics capture much of the essence of this phenomenon.

In the path of wave propagation there are obstacles such as trees, hills and buildings [10]. These obstacles scatter some of the wave along the path and the strength is reduced at the receiving point, as in [11] and [12]. It was mentioned that there are two main types of radar cross section, monostatic and bistatic.



**Figure 5.1** a typical wave propagation scenario.

Figure 5.1 illustrates how some of the scattered wave reaches the receiver and that some does also return to the transmitter. Since the hill is not perfectly conducting, one is concerned with the impedance aspect discussed in this report. For the sake of simplicity the surface impedance that describes the ground is assumed to be constant in space [13].

The scattering aspect of electromagnetic waves makes it relevant to relate some of the results obtained in this study to stealth technology. Stealth technology, also termed "low-observable" technology, is a set of techniques that render vehicles such as aircraft hard to observe. Since radar is the most difficult form of detection to elude, avoidance is generally accomplished by reducing the radar cross section (RCS) of the object to within the level of background noise. The reduction is done by shaping the target and by making a composite material that has a relative surface impedance close to one [5] [6] and [14]. As we have seen, this corresponds to near zero cross section for simple shapes and hence one is on the path to invisibility.

## VIII. CONCLUSION

Physical Optics (PO) was used to calculate the RCS of an imperfectly conducting sphere with an impedance boundary condition. Simulations using Matlab were done to verify the results. For high frequency Radar Cross Section computations, PO is numerically efficient for large targets. PO approximates the induced surface currents and by integration over the illuminated part of the scatterer, the method provides the scattered field. Targets that have impedance surfaces yield RCS results that are lower than the results of perfectly conducting surfaces. Therefore, the RCS of conducting targets can be decreased by material coating to reduce visibility. The PO results are in good agreement with exact results. The use of PO for impedance surfaces in the field of wave propagation is the application that is considered primarily here.

## REFERENCES

- [1] W. L. Stutzman, G. A. Thiele, *Antenna Theory and Design* (John Wiley & Sons Inc., Second Ed., 1998).
- [2] P. Uslenghi, "Radar cross section of imperfectly conducting bodies at small Wavelengths," *Alta Frequenza*, 33, 541-546, 1964.
- [3] D. K. Cheng, *Field and Wave Electromagnetics*, Second Ed., 1989.
- [4] D. W. Hill and Cha. C-C, "Physical optics approximation of the RCS of an impedance Surface," *IEEE AP*, 37, 416-419, 1988.
- [5] J. Rogers, L. Medgyesi-Mitschang, and J. Putnam, "Integral equation formulations for imperfectly conducting scatterers," *IEEE AP*, 33, 252 – 264, 1985.
- [6] E. F. Knott, J. F. Shaeffer, and M. T. Tuley, *Radar Cross Section*, Second Ed., 1993.
- [7] N. N. Youssef, "Radar cross section of complex targets," *Proc. IEEE*, 77, 722-734, 1989.
- [8] R. Kleinman, R. Goodrich and T. Senior, "Studies in radar cross sections: diffraction and scattering by regular bodies, the Sphere," Michigan university press, 1961.
- [9] MATLAB and Simulink Version 7.1, MAPLE manual version 10.
- [10] H. L. Bertoni, *Radio propagation for modern wireless systems*, Prentice Hall PTR, 2000.
- [11] J.H. Whitteker, "Fresnel-Kirchhoff theory applied to terrain diffraction problems," *Radio Science*, 25, 837-851, 1990.
- [12] G. Koutitas and C. Tzaras, "A UTD Solution for multiple rounded surfaces," *IEEE AP*, 54, 1277 - 1283, 2006.
- [13] F. Molinet, I. Andronov and D. Bouche, *Asymptotic and Hybrid Methods in Electromagnetics*, IEE Electromagnetics waves series 51, 2005.
- [14] E. F. Knott, "Aprogression of high-frequency RCS prediction techniques," *Proc. IEEE*, 73, 252 – 264, 1985.

## Appendix A1

```

%Radar Cross Section for Monostatic (Mie-Series) Ref. [5]
Freq1=1* 1e7
freq_steps = 130
c = 3e008 ;
iterations =100 ;
r=1

for k = 1 : freq_steps ;
    Freq = k* 1e7 ;
    Frequency( k ) = Freq ;
    lambda = c / Freq ;
    ka = 2 * pi * r / lambda ;
    kal(k)=ka;
    s = sqrt( pi / 2 / ka ) ;
    n = 1 : iterations ;
    [B1(n),ierr(1,n)] = besselj( n + 1/2, ka ) ;
    [B2(n),ierr(2,n)] = besselh( n + 1/2, 2, ka ) ;
    [B3(n),ierr(3,n)] = besselj( n + 1/2 - 1, ka ) ;
    [B4(n),ierr(4,n)] = besselh( n + 1/2 - 1, 2, ka ) ;
    if any(ierr)
        disp('Warning: There was an accuracy error in evaluating a Bessel or
        Hankel function.')
    end

    a(n) = ( s*B1 ) ./ ( s*B2 ) ;
    b(n) = ( ka * s*B3 - n .* s.*B1 ) ./ ...
        ( ka * s*B4 - n .* s.*B2 ) ;
    RCS = (lambda^2 / pi) * ( abs( sum( (-1).^n .* ( n + 1/2 ) .* ( b(n) -
    a(n) ) ) ) )^2 ;
    RCS1(k)=(RCS/pi/r^2)

end

plot( kal, RCS1,'-r','LineWidth',2 )
xlabel('ka ')
ylabel('\sigma /pi a^2 ')

```

### Appendix A2

```

%**** Equations 29, 31 for calculating the Monostatic RCS ****
zeta=0;
a=1;
theta=0;
phi=0;
rf=70;

%*****Where x = Theta_prime and y = Ph_prime ****

syms x y complex

for k=1:130
    ahat =[sin(phi) cos(phi)*cos(theta) cos(phi)*sin(theta)];
    bhat =[cos(phi) -sin(phi)*cos(theta) -sin(phi)*sin(theta)];
    khat =[0 sin(theta) -cos(theta)];
    nhat =[cos(y).*sin(x) sin(x).*sin(y) cos(x)];
    factor=(a.^2.*sin(x));

    nhat_dot_khat=dot(nhat,khat);
    nhat_dot_ahat=dot(nhat,ahat);
    nhat_dot_bhat=dot(nhat,bhat);

```

```

frequency=(k* 1e7 ) ;
frequency1(k)=frequency;
lambda=(3*1e8)/ frequency;
kwave=(2*pi)/lambda;
kwavel(k)=kwave*a;
part_1=nhat_dot_khat./(zeta.*nhat_dot_khat-1);
part_2=1+zeta.*nhat_dot_khat+2.*zeta.*(nhat_dot_ahat.^2./(nhat_dot_khat-zeta));
exponential=exp(2.*a.*i.*kwave.*(nhat_dot_khat));
g1=part_1*part_2*exponential*factor;
integeation1=vectorize(g1);
result1=dblquad(integeation1,0.003,pi/2,0,2*pi);
part_3=(nhat_dot_ahat.*nhat_dot_bhat)/((nhat_dot_khat-zeta).*(1-zeta.*nhat_dot_khat));
g2=nhat_dot_khat*part_3*exponential;
integration2=vectorize(g2);
result2=dblquad(integration2,0.003,pi/2,0,2*pi);
result3=2.*zeta.*result2;

% ***** in case of Equations 29 *****
% R=abs(rf-sqrt(rf-2.*rf.*cos(theta)));
% first_part=(i*exp(i*kwave.*R))./(lambda);
% E_scattered=first_part*(result1.*ahat+result3.*bhat);
% x_scattered=norm(E_scattered).^2;
% Encidant_field=ahat.*exp(a.*i.*kwave.*(sin(theta)-cos(theta)));
% y_Encidant=norm(Encidant_field).^2;
% sigma =4.*pi.*x_scattered./y_Encidant;
% sigmal(k)=sigma/pi;

% ***** in case of Equations 31 *****

x_scattered=abs(result1).^2+abs(result3).^2;
sigma =(4*pi./(lambda.^2)).*x_scattered;
sigmal(k)=sigma/pi
end

plot(kwavel,sigmal,'LineWidth',2)
xlabel('Ka ')
ylabel('\sigma /\pi a^2 ')

```

### Appendix A3

% \*\*\* Equation 28 for calculating the Bistatic and Monostatic cases

zeta=0;

a=1;

theta=0;

phi=pi/2;

% \*\*\*\*\*Where x = Theta\_prime and y = Ph\_prime \*\*\*\*\*

syms x y complex

% \*\*\*\*\* this is the case of calculating the Bistatic RCS

for k=1:3

max=k.\*pi/180;

theta\_o=max;

degree(k)=k;

% \*\*\*\*\* vector Parameters \*\*\*\*\*

```

ahat =[sin(phi) cos(phi)*cos(theta) cos(phi)*sin(theta)];
bhat =[cos(phi) -sin(phi)*cos(theta) -sin(phi)*sin(theta)];
khat =[0 sin(theta) -cos(theta)];
nhat =[cos(y). *sin(x) sin(x). *sin(y) cos(x)];

%***** in the case of calculating the Monostatic RCS then nnode=khat

nmod=[0 sin(theta_o) -cos(theta_o)];
b = cross(khat,nhat);
d=cross(nhat,b);
nhat_dot_khat=dot(nhat,khat);
nhat_dot_no_plus_khat=dot(nhat,(nmod+khat));
factor=(a.^2.*sin(x));
x_test=dot(nhat,khat)./(sqrt(b(1).^2+b(2).^2+b(3).^2).^2);
part_1=(dot(nhat,ahat)./(dot(nhat,khat)-zeta));
part_2= cross((nhat+(zeta*nmod)),b);
part_3= dot(ahat,b)./(dot(zeta*nhat,khat)-1);
part_4= b+(cross((zeta*d),nmod));

%***** fixing the value of the Frequency and K wave *****

frequency=(6.69* 1e8 );
frequencyl(k)=frequency;
lambda= 3*(10^8) / frequency;
kwave=(2*pi)/lambda;
kwavel(k)=kwave;
exponential=exp(a.*i.*kwave.*nhat_dot_no_plus_khat);
f_value=x_test*(part_1*part_2+part_3*part_4)*factor*exponential;

%***** to calculate the integration part *****

for h=1:3
    integration=vectorize(f_value(h));
    result(h)=dblquad(integration,0.003,pi/2,0,2*pi);
end

%***** to calculate the Scattered Field *****

R=50-a*cos(theta). *cos(theta_o);
first_part=(i*exp(i*kwave.*R))./(lambda);
E_scatared=first_part*result;
x_scatared=norm(E_scatared).^2;
tester(k)=x_scatared

%***** to calculate the Incident Field *****

Encidant_field=ahat.*exp(a.*i.*kwave.*(sin(theta)-cos(theta)));
y_Encidant=norm(Encidant_field).^2;

%***** To calculate the RCS*****

sigma =4.*pi.*x_scatared./y_Encidant;
signal(k)=(sigma)/(pi);
end

%***** To Plot the RCS*****

semilogy(degree,signal,'LineWidth',2)

```

xlabel('\theta (Degree)')  
ylabel('\sigma \wedge \pi a^2')